SANDIA REPORT
SAND2012-6748
Unlimited Release
Printed August 2012

Defect reaction network in Si-doped GaAs: Numerical predictions

Peter A. Schultz

Prepared by
Sandia National Laboratories
Albuquerque, New Mexico 87185 and Livermore, California 94550

Sandia National Laboratories is a multi-program laboratory managed and operated by Sandia Corporation, a wholly owned subsidiary of Lockheed Martin Corporation, for the U.S. Department of Energy's National Nuclear Security Administration under contract DE-AC04-94AL85000.

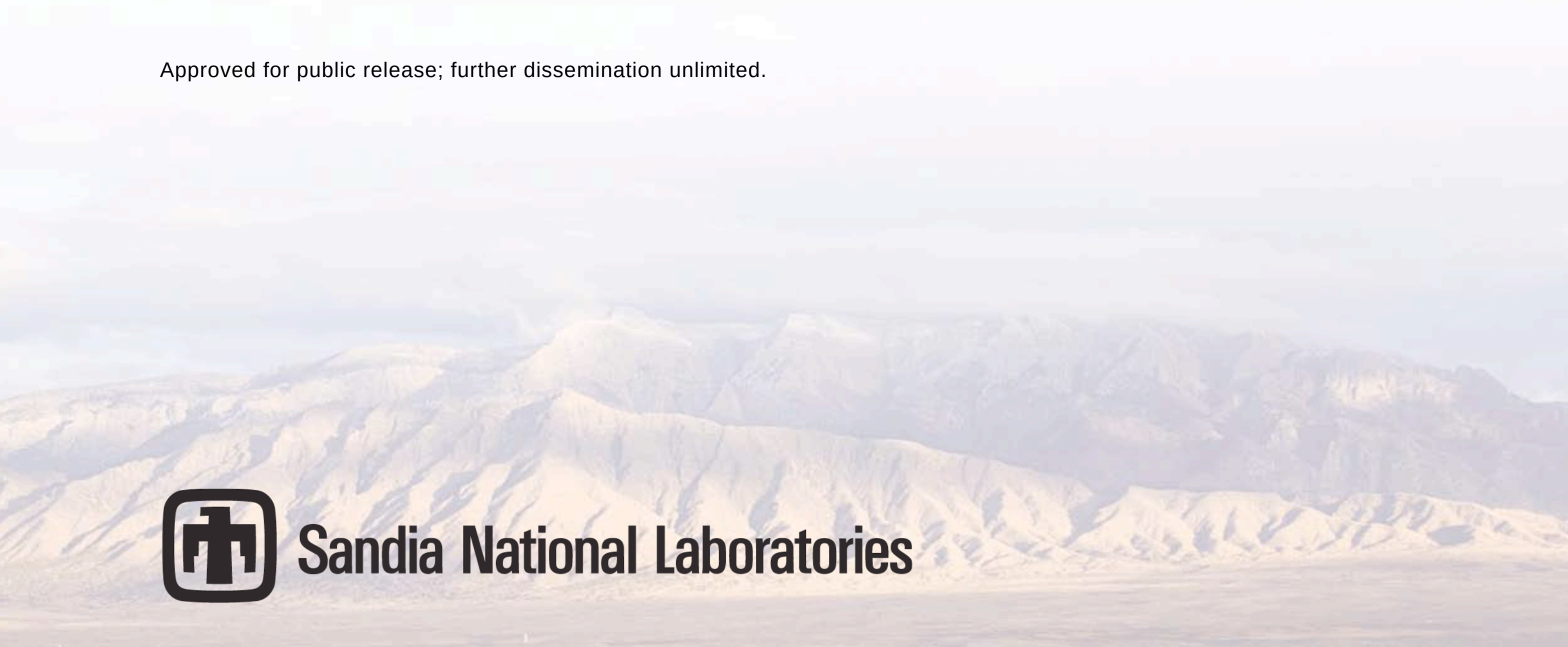

Sandia National Laboratories

Issued by Sandia National Laboratories, operated for the United States Department of Energy by Sandia Corporation.

Available to DOE and DOE contractors from
U.S. Department of Energy
Office of Scientific and Technical Information
P.O. Box 62
Oak Ridge, TN 37831

Telephone: (865) 576-8401
Facsimile: (865) 576-5728
E-Mail: reports@adonis.osti.gov
Online ordering: http://www.osti.gov/bridge

Available to the public from
U.S. Department of Commerce
National Technical Information Service
5285 Port Royal Rd.
Springfield, VA 22161

Telephone: (800) 553-6847
Facsimile: (703) 605-6900
E-Mail: orders@ntis.fedworld.gov
Online order: http://www.ntis.gov/help/ordermethods.asp?loc=7-4-0#online

SAND2012-6748
Unlimited Release
Printed August 2012

Defect reaction network in Si-doped GaAs: Numerical predictions

Peter A. Schultz
Advanced Device Technologies, Dept. 1425
Sandia National Laboratories
P.O. Box 5800
Albuquerque, New Mexico 87185-MS1322

Abstract

This Report characterizes the defect reaction network in silicon doped, *n*-type GaAs deduced from first principles density functional theory. The reaction network is deduced by following exothermic defect reactions starting with the initially mobile interstitial defects reacting with common displacement damage defects in Si-doped GaAs until culminating in immobile reaction products. The defect reactions and reaction energies are tabulated, along with the properties of all the silicon-related defects in the reaction network. This Report serves to extend the results for intrinsic defects in: P.A. Schultz and O.A. von Lilienfeld, “Simple intrinsic defects in GaAs”, Modelling Simul. Mater. Sci Eng., Vol. **17**, 084007 (2009) and its numerical supplement in SAND 2012-2675, and the preliminary silicon defect network results in: P.A. Schultz, “First-principles defect chemistry for modeling irradiated GaAs and III-V semiconductors”, J. Rad. Effects, Res. and Eng. Vol. **30**, p257 (2012).

This page intentionally left blank

CONTENTS

TABLES

NOMENCLATURE

CBE	conduction band edge
DFT	density functional theory
eV	electron Volt
FDSM	finite defect supercell model
GGA	generalized gradient approximation
LDA	local density approximation
LMCC	local moment countercharge
MSMSE	Modelling and Simulation in Materials Science and Engineering
n/x	not exist
PAS09	Article: P.A. Schultz and O.A. von Lilienfeld, MSMSE **17**, 084007 (2009).
PBE	Perdew/Burke/Ernzerhof, a “flavor” of GGA
PP	pseudopotential
SNL	Sandia National Laboratories
VBE	valence band edge

1. INTRODUCTION

The defect reaction network, the chain of reactions driven by species mobilized in primary displacement damage, is predicted and numerically characterized using first-principles density functional theory for irradiated silicon-doped, *n*-type gallium arsenide, GaAs. The reaction network is deduced from first principles: identifying the initial species mobilized during displacement damage, the arsenic and gallium interstitials, systematically investigating their reactions with dopants and immobile primary displacement damage defects and inserting into the network those reactions that are exothermic, and following this chain of reactions and potentially new mobile reaction products until culminating in immobile defects. The numerical predictions associated with this first-principles reaction network are presented in a series of numerical Tables containing parameters to populate defect physics packages needed for device simulations.

This Report focuses on silicon-containing defects in GaAs. Results for density functional theory (DFT) calculations of properties of simple intrinsic defects in gallium arsenide have been published previously in "Simple intrinsic defects in GaAs", P.A. Schultz and O.A. von Lilienfeld (2009), *Modelling and Simulation in Material Science and Engineering*, Vol. 17, Article # 084007 [1] (henceforth "PAS09"), and its supplement with numerical tables of intrinsic defect properties—charge transition defect level energies, formation energies, diffusion—published as a SAND Report [2]. Assessment of defect reaction network energies involving only intrinsic defects use values presented in these earlier works. The likely chain of defect reactions in carbon doped (*p*-type) and silicon doped (*n*-type) GaAs—the defect reaction networks—was presented previously [3], but properties of the defects in that network were not presented. This Report can be interpreted as a (partial, silicon-focused) numerical supplement to that work and as a numerical supplement to a paper yet to be published.

This Report focuses on first order reactions. Second order or greater (interstitial-interstitial, or interstitial-product) reactions are much less populous and unlikely to significantly affect electrical response of the bulk material, these reactions are therefore (mostly) neglected. Similarly, because *n*-type silicon doping will preferentially populate defects in their most negative charge states, emphasis is on careful characterization of defect evolution consistent with a Fermi level near the conduction band edge (although all accessible charge states for each defect in the network are examined).

1.1. Computational methods

The details of the computational methods are the same as comprehensively described previously [1,2,3], and will only be summarized here.

The DFT calculations are performed with the SEQQUEST code [4], using both the local density approximation (LDA) [5] and the Perdew-Burke-Ernzerhof (PBE) flavor of the generalized gradient approximation [6]. The comparison of LDA and PBE results is a partial assessment of the physical uncertainties within DFT functionals [7]. The pseudopotentials (PP) for Ga and As are the same used for intrinsic defects calculations [1,2] and comprehensively verified [8]. Calculations for the silicon-containing GaAs defects are done with 3*d*-core pseudopotentials (total valence charge *Z*=3) for the Ga atom, and not repeated with 3*d*-valence (*Z*=13) PP. We had determined that the PP construction had only modest effect on computed defect properties, the physical uncertainties in the DFT results dominated by the difference between the physical approximations of LDA and PBE [1]. If deemed necessary, the current calculations could be straightforwardly repeated using the more rigorous 3*d*-core PP for Ga. The silicon PP in this work are the same used and extensively validated in previous work for defects in bulk silicon [10]: generalized norm-conserving Hamann potentials [9], with a double-zeta plus polarization contracted-Gaussian basis set, as taken from the SEQQUEST library of optimized, transferable atomic potentials.

Defect formation energies are quoted in the arsenic-rich limit. The chemical potential of the As is set to the computed energy of the As in the elemental bulk *A7* structure, that of Ga to be that required to make the formation energy of perfect GaAs equal to zero. The chemical potential of a silicon atom is arbitrary, all reactions considered in this Report are silicon number conserving. Here, it is set to the energy of one atom in the crystalline diamond structure.

The calculations of charged defects use the Finite Defect Supercell Model (FDSM) [10] to incorporate rigorous boundary conditions for the solution of the electrostatic potential in a charged supercell [11,12] and extrapolate the computed defect energies to the infinitely dilute limit. Results for silicon related defects are presented for 216-site cubic supercells extrapolated to infinitely dilute limits, with selected 64-site and 512-site cubic supercells to verify these results are converged, as demonstrated in PAS09. The simulation contexts presented here correspond to the "LDA" and "PBE" simulation contexts defined in the numerical supplement for intrinsic defects [2].

One difference in the current calculations from the previous Reports [1-3] in these simulation contexts must be noted. The real space grids used in the original simulation contexts for calculations of intrinsic defects [1] proved inadequate to fully converge calculations with supercells containing carbon atoms. Rather than 108^3 grids used previously for the 216-site supercell calculations in the LDA and PBE simulation contexts, new carbon defects calculations required 144^3 grids (the same grids that had been found necessary for the LDA3d and PBE3d contexts). For consistency in developing the two reaction networks, the silicon defect calculations were also upgraded to the denser grid. Computed bulk properties and neutral defect formation energies are unaffected, to within 0.01 eV, with the finer grid. Mapping of computed ionization potentials to the valence band edge shifts (presented in Table 2 of PAS12) from 5.40 to 5.424 eV in the LDA context, and 5.15 to 5.172 eV in PBE, with the finer grid. With this adjustment, computed defect levels and formation energies of charged defects are also unaffected with the finer grid, to within 0.01 eV, the precision quoted in these reports.

1.2. Verification and validation

The silicon-related defect level calculations all use SEQQUEST and the FDSM, the same methods used in DFT calculations of defects in silicon, which yielded mean absolute errors of 0.1 eV and maximum absolute error of 0.2 eV for defect levels over a wide sampling of different defects in bulk silicon [10]. This is the expected accuracy (uncertainties) of the methods for defect level calculations in GaAs, and is the limit (best possible) of the physical accuracy of the DFT approximations used in this analysis.

Using the same methods and models, the verification and validation of the PP and extrapolation model inherit directly from earlier results for intrinsic defects in GaAs [1,2]. Validation of the overall computational method for GaAs defects is also done previously, indicating accuracy of 0.1 to 0.2 eV for defect level calculations in GaAs [1,2], and is not repeated here.

2. RESULTS

The section contains the Tables that summarize the numerical results for DFT simulations of silicon-related defects and the radiation-induced defect reaction network in GaAs.

The process by which the reaction network is deduced is iterative. It starts with the defects species generated by displacement damage (vacancies and interstitials). Using DFT calculations, we had identified that the self-interstitials and, particularly, the arsenic interstitial are mobile. Their reactions with all common immobile defects are investigated, and exothermic defect reactions are added to the reaction network. The “common” immobile defects are the vacancies and divacancy, being primary displacement damage defects, and the silicon dopant (substitutional) atoms. Reactions between mobile species, i.e., second order reactions, are neglected. One of the reaction products in the reaction network is the silicon interstitial Si_i, and the current results indicate Si_i might also be a mobile specie. Hence, its reactions with immobile defects are investigated, and the exothermic reaction products are added to the defect reaction network. No other reaction products are found that are likely to be mobile.

2.1. Defect atomic structures

The following Tables summarize the ground state structures for the silicon-containing defects within the defect reaction network. The intrinsic defect structures have been presented previously [1,2] and the same nomenclature is used to describe silicon defect structures as used in the intrinsic defects and illustrated in PAS09.

Table 1. Ground state structure description for silicon reaction network defects.

Charge state	**Si_{Ga}**	**Si_{As}**	**Si_i**	**$(Si_2)_{Ga}$**	**$(AsSi)_{Ga}$**	**Si_{vv}**
(4-)	-	-	-	-	-	C_{3v} Si_{As}-v_{Ga}
(3-)	-	-	-	-	-	C_{3v} Si_{As}-v_{Ga}
(2-)	-	-	split-110_{As} C_1 twisted [lda] C_{1h} [pbe]	C_2 split-110_{Ga} (001-twisted)	-	C_{1h} v_{Ga}-Ga_{As}-Si_{Ga} paired Si-Ga
(1-)	-	T_d	split-110_{As} C_1 twisted [lda] C_{1h} [pbe]	C_1 split-001_{Ga} di-puckered	-	C_{1h} v_{Ga}-Ga_{As}-Si_{Ga} paired Si-Ga
(0)	{T_d}[a]	{T_d}[a]	C_{1h} split-001_{Ga} pucker-Si [lda] C_{1h} 110_{Ga} [pbe]	C_{1h} split-110_{Ga}	C_{1h} Si_{Ga}— bridge-As[$T_{i,As}$]	C_{1h} v_{As}-Si_{Ga} paired Ga-Ga
(1+)	T_d	-	C_{2v} 001_{Ga} [lda] $T_{I,Ga}$ [pbe]	C_{3v} split-111_{Ga}	C_{1h} Si_{Ga}— bridge-As[$T_{i,As}$]	C_{1h} v_{As}-Si_{Ga} paired Ga-Ga
(2+)	-	-	$T_{I,As}$ [lda] $T_{I,Ga}$ [pbe]	C_{2v} split-001_{Ga} (to $T_{i,As}$) [lda] C_{3v} split-111_{Ga} [pbe]	C_{1h} split-001_{Ga} pucker-As [lda] C_{1h} As_{Ga}— bridge-Si[$T_{i,Ga}$]	C_{3v} v_{As}-Si_{Ga}

(a) The DFT result is not a defect state, but the state is in reality likely a shallow acceptor.

2.2. Defect charge transition energy levels

This section presents the defect charge transition levels of the silicon reaction network defects in GaAs, in eV, along with neutral formation energies. The defect level calculations are the fundamental result of this Report, the later formation energies and reaction energies are all derived from these results. The defect levels are thermodynamic values, differences in energies between global ground state structures of two charge states, without regard for whether a kinetic barriers might impede a structural rearrangement between the two atomic configurations.

Table 2. Defect levels for silicon reaction network defects, context = LDA.

LDA **Context**	**Neutral formation energy**	**Defect levels (eV), cf. VBE**						
		(3+/2+)	**(2+/1+)**	**(1+/0)**	**(0/1-)**	**(1-/2-)**	**(2-/3-)**	**(3-/4-)**
$Si_{Ga}^{(a,b)}$	**(1.93)$^{(a)}$**	n/x	n/x	(+2.52)$^{(a)}$	(+0.96)$^{(b)}$	n/x	n/x	n/x
Si_{Ga}	**0.95$^{(a)}$**	n/x	n/x	1.54$^{(a)}$	1.94$^{(b)}$	n/x	n/x	n/x
Si_{As}	**(2.36)$^{(a)}$**	n/x	n/x	n/x	(-0.49)$^{(a)}$	n/x	n/x	n/x
Si_i	**4.00**	n/x	1.14	0.83	1.50	1.40	n/x	n/x
$(Si_2)_{Ga}$	**4.04**	0.79	0.19	1.10	0.49	n/x	n/x	n/x
$(AsSi)_{Ga}$	**3.13**	n/x	0.19	0.51	-	-	n/x	n/x
Si_{vv}	**3.22**	n/x	0.62	0.38	0.93	0.69	1.30	1.51

(a) On-site Si_{Ga}(0) [Si_{As}(0)] is not a defect state in a DFT calculation. Energy quoted for Si_{Ga}[0] [Si_{As}(0)] is for the site-switched As_{Ga}-Si_{As} [Ga_{As}-Si_{Ga}] pair, and the (0/1+) [(0/1-)] transition energy between this neutral site-switched form and the charged substitutional.

(b) The Si_{Ga}(1-) is a 111-shifted *EL2*-like distorted state. It is not thermodynamically stable to emission of two electrons to the ground state substitutional Si_{Ga}(1+).

Table 3. Defect levels for silicon reaction network defects, context = PBE.

PBE **Context**	**Neutral formation energy**	**Defect levels (eV), cf. VBE**						
		(3+/2+)	**(2+/1+)**	**(1+/0)**	**(0/1-)**	**(1-/2-)**	**(2-/3-)**	**(3-/4-)**
$Si_{Ga}^{(a,b)}$	**(1.79)$^{(a)}$**	n/x	n/x	(2.43)$^{(a)}$	(1.10)$^{(b)}$	n/x	n/x	n/x
Si_{Ga}	**0.90$^{(a)}$**	n/x	n/x	1.54$^{(a)}$	1.99$^{(b)}$	n/x	n/x	n/x
Si_{As}	**(2.38)$^{(a)}$**	n/x	n/x	n/x	(-0.47)$^{(a)}$	n/x	n/x	n/x
Si_i	**3.86**	n/x	1.40	0.57	1.57	1.49	n/x	n/x
$(Si_2)_{Ga}$	**3.91**	0.86	0.16	1.14	0.53	n/x	n/x	n/x
$(AsSi)_{Ga}$	**3.03**	n/x	0.30	0.62	-	-	n/x	n/x
Si_{vv}	**3.07**	n/x	0.83	0.45	1.00	0.69	1.42	1.50

(a) On-site Si_{Ga}(0) [Si_{As}(0)] is not a defect state in a DFT calculation. Energy quoted for Si_{Ga}[0] [Si_{As}(0)] is for the site-switched As_{Ga}-Si_{As} [Ga_{As}-Si_{Ga}] pair, and the (0/1+) [(0/1-)] transition energy between this neutral site-switched form and the charged substitutional.

(b) The Si_{Ga}(1-) is a 111-shifted *EL2*-like distorted state. It is not thermodynamically stable to emission of two electrons to the ground state substitutional Si_{Ga}(1+).

The first entry for Si_{Ga} in the tables is the explicit DFT calculated result, and the second entry is for the physical prediction. Silicon is a shallow *n*-type dopant in GaAs, sitting in the gallium substitutional site, Si_{Ga}. Being a shallow donor, Si_{Ga} has a (1+/0) transition near the valence band edge. However, the DFT calculation buries this state deep in the conduction band and the Si_{Ga}[0] (and its compensating partner Si_{Ga}[0]) is not a clean defect state. To evaluate a formation energy for Si_{Ga}[1+], a clean neutral defect state is needed. A neutral reference state is obtained by swapping the silicon and a neighboring gallium, a defect pair which does have a clean defect state with neutral charge. With this neutral defect and the charge transition energy, the formation energy of Si_{Ga}[1+] (and Si_{As}[1-]) is obtained directly from the DFT calculations, without assumptions regarding the location of the (computationally inaccessible) shallow on-site transition.

The *DX* center, the Si_{Ga}[1-], is a true defect state in its 111-offset configuration. It is not thermodynamically stable (to a double-emission to the Si_{Ga}[1+] donor state).

The computed levels in the LDA and PBE contexts are very similar, all within 0.2 eV of one another, and mostly within 0.1 eV. This similarity is despite differences in defect formation energies that are typically 0.2 eV or more, and is, first, evidence that electronic transition levels are benefitting from a cancellation of errors and, second, consistent with and evidence for a physical uncertainty in defect levels of 0.1-0.2 eV.

The levels listed in these tables only quote those charge states that are thermodynamically accessible. For example, clean defect states for the $(AsSi)_{Ga}$ can be found for [1-] and [2-] charge states and a *DX* (offset-Si) configuration for Si_{Ga}, is a clean defect state as a [1-], but none of these is thermodynamically stable, all will spontaneously emit electrons to form the neutral defects. Alternatively stated, the electronic levels are above the CB edge, as a consequence of the structural rearrangements that occur.

2.3. Defect formation energies

The ground state defect formation energies, as a function of charge state are trivially obtained by simple arithmetic from the neutral formation energies and the computed defect charge transition energy levels in the previous section. As for all the results presented in this Report, the defect formation energies in these Tables are presented in the arsenic-rich limit. The formation energies of the charged defects are presented with the Fermi level at the VBE. The Tables present the formation energies of the silicon reaction network defects, segregated by simulation context. Only thermodynamically accessible charge states are listed.

Table 4. Formation energies of silicon reaction network defects at VBE (in eV), context = LDA.

Charge state	**Si_{Ga}**	**Si_{As}**	**Si_i**	**$(Si_2)_{Ga}$**	**$(AsSi)_{Ga}$**	**Si_{vv}**
(4-)	-	-	-	-	-	7.66
(3-)	-	-	-	-	-	6.14
(2-)	-	-	6.90	-	-	4.84
(1-)	(2.89)(a)	1.87	5.50	4.52	-	4.15
(0)	**(0.95)(b)**	**(0.33)(b)**	**4.00**	**4.04**	**3.13**	**3.22**
(1+)	-0.59	-	3.17	2.93	2.62	2.83
(2+)	-	-	2.03	2.75	2.43	2.22
(3+)	-	-	-	1.96	-	-

(a) For a C_{3v} distorted Si_{Ga}[1-], assuming a shallow donor level exactly at the CB edges.

(b) For a T_d on-site Si_{Ga}[0] and Si_{As}[0], assuming a shallow level exactly at the respective edges. Note difference from the neutral formation energy in Table 1 defect level calculations.

Table 5. Formation energies of silicon reaction network defects at VBE (in eV), context = PBE.

Charge state	**Si_{Ga}**	**Si_{As}**	**Si_i**	**$(Si_2)_{Ga}$**	**$(AsSi)_{Ga}$**	**Si_{vv}**
(4-)	-	-	-	-	-	7.68
(3-)	-	-	-	-	-	6.18
(2-)	-	-	6.91	-	-	4.76
(1-)	(2.89)(a)	1.91	5.42	4.45	-	4.07
(0)	**(0.90)(b)**	**(0.37)(b)**	**3.86**	**3.91**	**3.03**	**3.07**
(1+)	-0.64	-	3.29	2.77	2.41	2.62
(2+)	-	-	1.89	2.61	2.11	1.79
(3+)	-	-	-	1.75	-	-

(b) For a C_{3v} distorted Si_{Ga}[1-], assuming a shallow donorlevel exactly at the CB edges.

(a) For a T_d on-site Si_{Ga}[0] and Si_{As}[0], assuming a shallow level exactly at the respective edges. Note difference from the neutral formation energy in Table 1 defect level calculations.

2.4. Silicon interstitial and migration

In the evolution of the defect reaction network, as the mobile As and Ga interstitials react with the immobile fixed defects, the silicon interstitial is the only defect that shows the prospect to be also mobile, and therefore must be considered in extending the defect reaction network.

2.4.1. *Silicon interstitial structural energies*

The following Table presents the relative energies of different structures of the silicon interstitial relative to the ground state structure for that charge state. This is not a comprehensive listing of possible structures considered, but does survey all the potentially important structures for Si_i.

Table 6. Silicon interstitial ground state energies, in eV, context = LDA

		Energy relative to ground state structure				
Structure	Context	Si_i(2-)	Si_i(1-)	Si_i(0)	Si_i(1+)	Si_i(2+)
C_{1h} split-001$_{Ga}$ pucker-Si ("p-Si")	LDA	CB	CB	0.02	—> $T_{i,Ga}$	-
C_{1h} split-001$_{Ga}$(p-Ga)	LDA	0.91	0.72	0.40	-	-
C_{2v} split-001$_{Ga}$	LDA	CB	CB	1.26	0.90	1.32
C_{3v} split-111$_{Ga}$	LDA	CB	CB	0.54	—> $T_{i,Ga}$	0.68
C_{1h} split-111$_{Ga}$ bent bridge (to $T_{i,As}$)	LDA	CB	CB	0.33	0.43	—> C_{3v}
C_{1h} split-111$_{Ga}$ bent bridge (to $T_{i,Ga}$)	LDA	CB	CB	0.02	—> $T_{i,Ga}$	-
C_{1h} split-110$_{Ga}$	LDA	CB	CB	**0**	0.21	—> 111
C_{1h} split-001$_{As}$ (p-As)	LDA	CB	CB	0.08	0.50	—> BC
C_{1h} split-001$_{As}$ (p-Si)	LDA	CB	CB	—> *H*	0.19	—> $T_{i,As}$
C_{2v} split-001$_{As}$	LDA	CB	CB	0.57	0.55	1.09
C_{1h} bent As-bridge (to $T_{i,Ga}$)	LDA	0.10	0.11	0.51	–> 001$_{As}$	-
C_{1h} split-110$_{As}$	LDA	**0**	**0**	0.22	0.46	—> $T_{i,As}$
C_1 split-110$_{As}$ twisted	LDA	—> C_{2v}	—> C_{2v}	—> C_{2v}	-	-
C_{3v} Bond-Center	LDA	1.01	0.87	1.02	0.74	1.02
C_{3v} H-site interstitial	LDA	-	-	0.40	0.47	1.21
C_{3v} off-$T_{i,As}$ -site	LDA	-	-	—> *H*	0.20	0.08 (T_d)
T_d $T_{i,Ga}$-site	LDA	-	-	0.44	**0**	**0**

Table 7. Silicon interstitial ground state energies, in eV, context = PBE

		Energy relative to ground state structure				
Structure	Context	Si_i(2-)	Si_i(1-)	Si_i(0)	Si_i(1+)	Si_i(2+)
C_{1h} split-001_{Ga} pucker-Si ("p-Si")	PBE	CB	CB	**0**	—> $T_{i,Ga}$	-
C_{1h} split-001_{Ga}(p-Ga)	PBE	CB	CB	CB	-	-
C_{2v} split-001_{Ga}	PBE	CB	CB	1.17	0.51	1.08
C_{3v} split-111_{Ga}	PBE	CB	CB	0.47	—> $T_{i,Ga}$	0.51
C_{1h} split-111_{Ga} bent bridge (to $T_{i,As}$)	PBE	CB	CB	0.37	0.12	—> C_{3v}
C_{1h} split-111_{Ga} bent bridge (to $T_{i,Ga}$)	PBE	CB	CB	—> p-Si	—> $T_{i,Ga}$	-
C_{1h} split-110_{Ga}	PBE	CB	CB	0.11	**0**	—> $T_{i,Ga}$
C_{1h} split-001_{As} (p-As)	PBE	CB	CB	0.10	0.20	—> BC
C_{1h} split-001_{As} (p-Si)	PBE	CB	CB	—> *H*	—> $T_{i,As}$	—> $T_{i,As}$
C_{2v} split-001_{As}	PBE	CB	CB	0.57	0.25	1.09
C_{1h} bent As-bridge (to $T_{i,Ga}$)	PBE	0.01	0.06	0.51	0.44	-
C_{1h} split-110_{As}	PBE	0.02	0.03	0.26	0.18	—> $T_{i,As}$
C_1 split-110_{As} twisted	PBE	**0**	**0**	—> p-As	-	-
C_{3v} Bond-Center	PBE	CB	CB	1.09	0.48	0.96
C_{3v} H-site interstitial	LDA	-	-	0.49	0.19	1.09
C_{3v} off-$T_{i,As}$ -site	LDA	-	-	CB	CB	**0** (T_d)
T_d $T_{i,Ga}$-site	LDA	-	-	CB	CB	0.04

The LDA and PBE structural landscapes for the silicon interstitial are similar, particularly for the negative charge states that will be prevalent in the *n*-type Si-doped GaAs. The PBE results tend to have more states that rise into the conduction band rather rather than be defect states, but the ground state structures are mostly unaffected. The silicon strongly favors in-network sites when negatively charged, and the non-bonding interstitial sites when positively charged.

2.4.2. Silicon interstitial diffusion

There will be little or no thermal diffusion of Si in negative charge states that the Si will normally populate in *n*-type doping. The Si favors in-network bonds strongly in *n*-type, and prefers the split-As site over the split-Ga site. Diffusion must go by hopping from site to site, in-network. The Ga-site Si-interstitial sites along any viable diffusion pathway are ~1 eV higher than the As-site split-interstitial ground state configurations, precluding diffusion at any reasonable operating temperature. Computation of continuous pathways and explicit barriers for the diffusion of the negative interstitial is impractical using a local functional, because of extensive regions where the defect state crosses into the conduction band, but also is unnecessary given the strong preference for the As site and lack of low-energy intermediate sites.

Unlike for the arsenic interstitial [1], there is not an identified path that enables athermal migration [13] of the silicon interstitial via a Bourgoin-Corbett mechanism [14], in either the LDA or PBE context simulations. There is the possibility for strongly recombination(current)-enhanced diffusion among the positive charge states up to the neutral, and perhaps there is a mechanism for net athermal migration in the positively charged silicon interstitial, but these charge states will be very infrequently populated in the *n*-type material created by the Si-doping, and diffusion by this mechanism is unlikely to contribute to defect evolution in radiation damaged GaAs.

Although there is no obvious mechanism for athermal diffusion, there is, nonetheless, the prospect for recombination-enhanced diffusion. Upon capture of two minority carriers (holes) to become a neutral Si_i[0], there is much greater potential for thermal migration. The relatively flat landscape with multiple low-energy structure (within ~0.5 eV) of the ground state—in-network sites on both the As and Ga sites and competitive off-network interstitial sites—suggests that diffusion might be relatively facile, particularly after capture of two carriers, each depositing some energy in vibrational modes. Whatever mobility exhibited by the Si interstitial is likely to occur through this recombination-enhanced mechanism.

2.5. Defect network reaction energies

Using the defect formation energies tabulated above for the silicon-related defects, and the defect formation energies previously tabulated for intrinsic defects [2], it is straightforward to compute the defect reaction energies of possible reactions in the defect reaction network for Si-doped GaAs. All reactions of the three potentially mobile species, the arsenic and gallium self-interstitials and the silicon interstitials, with the common immobile defects, the vacancies and dopants are considered. The reaction energies among intrinsic defects are summarized in a companion report on the carbon reaction network [15]. The results for charge conserving reaction for the remaining silicon-containing reactions are presented in the following Table.

Table 8. Defect reaction energies, in eV.

Charge conserving defect reaction						Reaction energy[(a)]	
Reactant defects				Product defect		Simulation context	
Mobile specie	charge	Immobile target	charge	Defect	charge	LDA	PBE
As_i	-1	Si_{Ga}	+1	$(AsSi)_{Ga}$	0	-0.70	-0.67
As_i	-1	Si_{As}	-1	Si_i	-2	+0.61	+0.66
Ga_i	+1	Si_{Ga}	+1	Si_i	+2	+0.36	+0.35
Si_i	0	v_{Ga}	+1	Si_{Ga}	+1	-6.94	-6.55
Si_i	0	v_{As}	-1	Si_{As}	-1	-6.25	-6.06
Si_i	0	vv	0	Si_{vv}	0	-4.97	-4.38
Si_i	0	As_{Ga}	0	$(AsSi)_{Ga}$	0	-2.37	-2.10
Si_i	0	Si_{Ga}	+1	$(Si_2)_{Ga}$	+1	-0.48	-0.45

(a) A negative energy denotes exothermic (downhill) reaction.

Note that the direction of the charge-conserving reactions does not necessarily align with the thermodynamic reaction. In particular, while the Ga_i+Si_{Ga}–>Si_i is uphill in charge-conserving form, it is downhill thermodynamically for a Fermi level at the CB edge (i.e., allowing for the capture of carriers appropriate to that Fermi level). Additionally, a number of the reaction energies are small enough to be possibly reversible, and including this reversibility might be desired in device simulations.

3. CONCLUSIONS

The defect reaction network for *n*-type silicon doped gallium arsenide is developed, beginning with the interstitials mobilized in displacement damage, following the reactions with the immobile displacement damage defects and the dopant atoms, and culminating in immobile reaction products. The defect reaction energies computed with DFT are presented for each reaction in the network, and the computed properties needed to describe the each defect in the network—stable charge states, energy levels, formation energies—are tabulated. Both LDA and PBE results are presented. The results are only presented using “large-core” Z=3 Ga pseudopotentials. The calculations could be straightforwardly repeated with the small-core Z=13 Ga pseudopotentials.

4. REFERENCES

1. P.A. Schultz and O.A. von Lilienfeld, Modelling Simul. Mater. Sci. Eng. **17**, 084007 (2009).
2. P.A. Schultz, “Simple intrinsic defects in GaAs: Numerical Supplement”, SAND2012-2675, Sandia National Laboratories, Albuquerque, NM, April 2012. [Unclassified]
3. P.A. Schultz, J. Rad. Effects Research and Engineering **30**, 257 (2012).
4. SEQQUEST code, unpublished, http://dft.sandia.gov/quest/
5. J.P. Perdew and A. Zunger, Phys. Rev. **23**, 5048 (1981).
6. J.P. Perdew, K. Burke, and M. Ernzerhof, Phys. Rev. Lett. **77**, 3865 (1996).
7. A.E. Mattsson, P.A. Schultz, M.P. Desjarlais, T.R. Mattsson, and K. Leung, Modelling Simul. Mater. Sci. Eng. **13**, R1 (2005).
8. O.A. von Lilienfeld and P.A. Schultz, Phys. Rev. B **77**, 115202 (2008).
9. D.R. Hamann, Phys. Rev. B **40**, 2980 (1989).
10. P.A. Schultz, Phys. Rev. Lett. **96**, 246401 (2006).
11. P.A. Schultz, Phys. Rev. B **60**, 1551 (1999).
12. P.A. Schultz, Phys. Rev. Lett. **84**, 1942 (2000).
13. G.D. Watkins, in *Radiation Damage in Semiconductors*, ed. P. Baruch, p97 (Paris:Dunod, 1965).
14. J.C. Bourgoin and J.W. Corbett, Phys. Lett. A **38**, 135 (1972).
15. P.A. Schultz, “Defect reaction network in C-doped GaAs: Numerical predictions”, SAND2012-6659, Sandia National Laboratories, Albuquerque, NM, August 2012. [Unclassified]

DISTRIBUTION

(to be distributed electronically)

1	MS0899	Technical Library	9536 (electronic copy)
1	MS1179	L. J. Lorence	1341 (ljloren@sandia.gov)
1	MS1056	W. R. Wampler	1111 (wrwampl@sandia.gov)
1	MS1323	E. R. Keiter	1445 (erkeite@sandia.gov)
1	MS1315	J. S. Nelson	1131 (jsnelso@sandia.gov)
1	MS1189	T. R. Mattsson	1641 (trmatts@sandia.gov)
1	MS0457	R. A. Paulsen	2211 (rapauls@sandia.gov)
1	MS1415	A. F. Wright	1131 (afwrigh@sandia.gov)

Sandia National Laboratories